

Possible New Pointing Models for the GBT: Definitions and Comparisons

Ellie White, Frank Ghigo, David Frayer, Ron Maddalena, Patrick Wallace

April 26, 2022

File: PROJECTS

Keys: PTCS, TPOINT

Abstract

According to recent analyses, with the 5s pointing model, the GBT is capable of achieving 9 arcsecond RMS blind pointing accuracy during nighttime observing, 5 arcsecond RMS all-sky relative pointing, and as good as 1.2 arcseconds RMS pointing accuracy when a calibration is performed within 1 hour and 10° of the target source. The 5s model was created in fall of 2016, using 2016 and pre-2016 pointing run data. We wanted to find out if adding or removing terms from the 5s model, and fitting to a 2017-2018 data set, would improve the model's present-day performance in any of the metrics given above. To this end, we have completed several experiments utilizing TPOINT to compare the performance of a variety of models; after creating models by fitting them to the 2017-2018 data set, we compared their performance on newly-acquired 2021 pointing run data, keeping all coefficients of the models fixed as they would be if the models were applied during an actual observing run. A few of the new models we tested showed improvements in all sky relative pointing performance, but most new models did not show visible improvements over the 5s model. We present here a summary of these results so that they can inform future modeling experiments and attempts to improve upon the GBT's current model.

Contents

1. Introduction	3
2. Selection and pre-processing of pointing runs	3
3. TPOINT fitting and initial comparison of new models	4

3.1. Definitions	5
3.2. Summary of pointing models	5
3.3. Summary of model-fitting results	7
4. Comparison of pointing models' performance on 2021 data	8
5. Conclusions	8
6. Acknowledgements	9

History

80.1: April 26, 2022. Original version (Ellie White).

1. INTRODUCTION

While the GBT can currently achieve blind pointing to an accuracy of about 9 arcseconds during nighttime observing, to achieve peak pointing performance, observers are required to make adjustments at the beginning of each observing session. The observer must perform a preliminary pointing scan to determine elevation and cross-elevation pointing errors that remain after applying the general pointing model. These errors are corrected by applying local pointing corrections (LPCs); once these corrections are applied at the beginning of a session, pointing errors for the rest of the run are minimal; if one scan is performed at the beginning of an all-sky observing session, the RMS error is reduced to 5 arcseconds, and if a calibration is performed within 10° of the source and within 1 hour of starting the observation, errors as low as 1.2 arcseconds can be achieved [1].

We wanted to determine if we can lower any of these errors by implementing a different pointing model. We retrieved 754 calibration scans from pointing runs spanning January 2017 through December 2018 and used this data set to fit different models with TPOINT. In section 2, we'll present the set of steps we went through to pre-process the 2017-2018 datasets to make them compatible with TPOINT and perform quality control to remove corrupted scans. We will describe the different test models and their respective performance when fit to the 2017-2018 data sets in section 3. In section 4, we will present the results of applying each of the models described in section 3 to a 2021 pointing run, and finally, in section 5 we will provide our conclusions and recommendations for which pointing model to implement moving forward.

2. SELECTION AND PRE-PROCESSING OF POINTING RUNS

Before the pointing run data could be analyzed using TPOINT, it was necessary to identify pointing runs or observing runs containing a large number of calibration scans in the GBT data archives. We selected 14 (purely X-Band) pointing runs for analysis, as summarized in Table 1.

These pointing sessions had to be pre-processed to achieve two functions: (1) performing quality control measures to remove any jack scans corrupted by wind or other inclement conditions from the data set, and (2) creating a TPOINT-compatible input file for each observing session¹.

Note that each calibration scan consists of four individual peak scans (two in elevation and two in cross-elevation) taken of the same bright, unresolved source. The criteria for keeping or rejecting an individual scan are determined based on the assumption that the shape of each peak scan approximates a Gaussian with a FWHM determined by the frequency at which the observation was taken. If the properties of the predicted Gaussian (e.g. FWHM, height, central offset) don't agree well with the properties of a Gaussian that is fit to the actual peak scan, or if two scans in the same direction (e.g., both elevation scans) don't agree well with each other (thresholds summarized in Table 2), the scan is assumed to be corrupted by wind, poor weather, etc. and thus removed from the dataset [2]. Only one scan was rejected as a result of applying these heuristics.

¹ For details on the software we used to preprocess this data, and for instructions on how to reproduce our steps, see this Wiki page: <https://safe.nrao.edu/wiki/bin/view/GB/PTCS/PointingSoftwareDocs>

Session ID	Number of Scans	Subset Label
TPTCSPNT_170105	46	A
TPTCSRMP_170107	10	B
TPTCSPNT_170109	78	C
TPTCSPNT_170917	41	D
TPTCSPNT_170920	74	E
TPTCSPNT_171126	76	F
TPTCSPNT_180509	23	G
TPTCSPNT_180511	55	H
TPTCSPNT_180520	10	I
TPTCSPNT_180526	79	J
TPTCSPNT_180821	148	K
TPTCSPNT_181212	58	L
TPTCSPNT_181219	37	M
TPTCSPNT_181220	19	N

Table 1. List of pointing runs used for analysis. Number of scans is counted after the removal of corrupted scans.

Heuristic	Rejection Threshold
FWHM	50%
Height	50%
Central offset	300%

Table 2. For row 1, if a calibrator scan’s measurements differed from a predicted Gaussian shape by more than the percentage given, then the scan was rejected in pre-processing. Similarly, for rows 2 and 3, if the height and central offset of two scans taken in the same direction (of the same source) differed by more than the percentages given, the scan was rejected.

A large part of the analysis done in this project consisted of assessing the effects of including additional metrological terms in the TPOINT modelling, such as raw temperature sensor readings and inclinometer measurements in addition to the terms that are already part of the model (such as the Constantikes temperature calculations and the calculated inclinometer terms). To incorporate these additional measurements, the preprocessing program **utpmake** was modified to include these fields in the TPOINT input files².

3. TPOINT FITTING AND INITIAL COMPARISON OF NEW MODELS

TPOINT is a software package that can be used to assess a telescope’s overall pointing performance, identify mechanical effects which cause systematic pointing errors, and create pointing models to minimize pointing errors as much as possible in order to improve blind pointing

² A list of the fields included in the TPOINT input file can be accessed here: <https://safe.nrao.edu/wiki/bin/view/GB/PTCS/TpointKey>

accuracy and reduce wasted overhead time trying to locate the target object [3]. TPOINT contains a number of features which proved useful in our analysis: it allows the user to load in single data files or several data files at once for simultaneous analysis, apply models with pre-set terms to the given data sets, create models by fitting individual model terms to data sets, use subsets to allow terms to be fit differently to individual observing runs within an overall data set, and plot the results of the analysis for the user's benefit. We used these features of TPOINT to complete our comparison of several models.

3.1. Definitions

Before describing the models that were created and their performance, it is important to make note of some definitions and conventions in use at the GBT. As described in [1], the pointing model is represented by the difference between the two coordinate frames:

$$\Delta X_{EL} = \Delta(AZ) * \cos(EL_{mnt}) = (AZ_{mnt} - AZ_{obs}) * \cos(EL_{mnt}) \quad (1)$$

$$\Delta EL = EL_{mnt} - EL_{obs} \quad (2)$$

where cross-elevation (X_{EL} , or $AZ * \cos(EL)$) is used instead of azimuth in the formulation of the model. The terms with subscript "mnt" refer to the encoder coordinates, while the terms with subscript "obs" refer to the coordinates of the object on the sky. Note also that at the GBT, azimuth is measured from north to east.

3.2. Summary of pointing models

Below is a summary of the different pointing models we created and compared; please note that the models themselves and the methods we used to fit them are all included in this Wiki page: <https://safe.nrao.edu/wiki/bin/view/GB/PTCS/2020PointingModelComparison>. See Table 6 for definitions of the TPOINT terms mentioned in each model description below.

- **Standard Model:** the 5s GBT pointing model, which was in use up until January of 2021, when it was replaced by the 5u model, which is almost identical with the exception of changes to the values of two track coefficients. We chose to use the 5s model for this analysis because the 2017-2018 data we fit the models on was obtained using the 5s model. See Figures 1, 2, and 3 for scatter plots showing the performance of the Standard Model.
- **Standard Model with no auxiliary terms:** the GBT 5s pointing model, minus the standard inclinometer and Constantikes temperature terms. Note that when we refer to **Constantikes temperature terms**, we are referring to the calculated temperature terms currently included in the GBT's model, which are different from the raw temperature terms included in some models; Table 7 summarizes the location of each temperature sensor, and Table 8 lists the equations used to calculate each Constantikes temperature term [4].

- **Standard Model with no inclinometer terms:** the GBT 5s pointing model, minus the standard inclinometer terms (in Table 6, the standard inclinometer terms correspond to A12E, A13V, and A14A, and the λ values are calculated from the inclinometers as shown in Table 9).
- **Standard Model, no Constantikes temperature terms:** the GBT 5s pointing model minus the Constantikes temperature terms.
- **Standard Model with temperature sensors:** the GBT 5s model with the addition of terms corresponding to all of the GBT's raw temperature sensors in addition to the Constantikes temperatures.
- **Standard Model with temperature sensors but no Constantikes temperature terms:** the GBT 5s model with the addition of terms corresponding to all of the GBT's raw temperature sensors but excluding the Constantikes temperature terms.
- **Standard Model with temperature sensors and raw inclinometers:** the GBT 5s model with the addition of terms corresponding to all of the GBT's raw temperature sensors and raw inclinometer readings in addition to the Constantikes temperatures and standard inclinometer terms.
- **Standard Model with raw inclinometers:** the GBT 5s model with the addition of terms corresponding to raw inclinometer readings in addition to the standard, calculated inclinometer terms.
- **Standard Model minus four auxiliary terms:** the GBT 5s model without four auxiliary terms (A11A, A5E, A4S, and A3S) which appear to be statistically insignificant based on the fact that the error values associated with determining these coefficients are comparable to the values of the coefficients themselves.
- **Standard Model, MVET'ed:** TPOINT has a command – MVET – which uses the Akaike information criterion to identify and remove the weakest terms in the model. We created a model by running MVET on the GBT 5s model, and thus removing the terms A14A, A4S, A9E, A5E, A3S, A2S, HESA, and HSSE. See Figures 4, 5, and 6 for scatter plots showing the performance of the MVET'ed model.
- **Model P1:** Contains no auxiliary terms; only geometric terms IA, IE, HASA4, HECA, HESA2, HECA2, HESA3, HECA8, HESE, HESE2, NPAE, CA, AN, AW, TF (see section 7 of the TPOINT manual for the physical meanings of the terms not listed in Table 6 [3]; note that for terms beginning with the letter H, the functional form is encoded in the term name, following TPOINT conventions).
- **Model P2:** Again, no auxiliary terms, only geometric terms IA, IE, HASA2, HASA4, HASA8, HESA, HESA2, HESA3, HECA3, HECA8, HESE, HECE3, HECE6, HESE7, HECE7, HVSA3, NPAE, CA, HSCA, AN, AW, TF.
- **Model P3:** Includes geometric and auxiliary terms IA, IE, A14A, HASA, HASA4, A6E, A7E, A12E, HECA, HESA2, HECA2, HESA3, HECA3, HESE, HECE5, HESE8, A10V, A13V, NPAE, CA, HSSA, AN, AW, TF.

Model Name	RMS	POP STD
Standard Model	6.64	6.74
Standard mod., no aux.	9.47	9.52
Standard mod., no incl. terms	8.93	8.98
Standard mod., no Constantikes temps.	9.30	9.35
Standard mod. with raw temp. sensors	4.78	5.20
Standard mod. with raw temperature sensors but no Constantikes temps	4.85	5.23
Standard mod. with raw temp. sensors and raw incl.'s	4.66	5.15
Standard mod. with raw incl.'s	6.29	6.47
Standard Model minus four aux. terms	7.59	7.68
Standard Model, MVET'ed	8.13	8.20
P1 – no aux, some geom.	8.65	8.73
P2 – no aux, more geom.	8.50	8.61
P3 – some aux, some geom.	7.84	7.96
P4 – more aux., more geom.	8.30	8.49

Table 3. Summary of blind pointing performance of models on 2017-2018 data sets. Note RMS = root mean square and POP STD = population standard deviation.

- **Model P4:** Includes geometric and auxiliary terms IA, IE, A14A, HASA, HACA, HASA2, HASA4, HASA7, HASA8, A12E, HESA, HESACE, HECA, HESA2, HECA2, HESA3, HECA3, HECA8, HECE2, HESE7, HECE7, HESE8, HECE8, A10V, A13V, NPAE, CA, A2S, A4S, HSSA, AN, AW, TF, TX10.

3.3. Summary of model-fitting results

To create models for subsequent testing on the 2021 data set, we loaded in each of the models described above, one at a time, along with the 2017-2018 data set, and then ran TPOINT's FIT command to see how well each model could be fit to the data, and what resulting RMS each one would produce. The results are summarized in Tables 3 and 4; Table 3 shows the performance you would see on 2017-2018 data with the models fit to the whole data sets without adjustment, and Table 4 shows the performance you would see if you gave each pointing session its own offsets, simulating a calibration at the beginning of the run. Since the pointing runs in the 2017-2018 data set are all-sky, Table 4 essentially gives the all-sky relative pointing performance you would see with each new model.

Note that although models like the Standard Model already existed with set coefficients, in order to create more current models, we allowed TPOINT to fit the coefficients to find the best values for the 2017-2018 data. It is also worth pointing out that for models with a large number of additional terms (for example, those that include a term for each raw temperature sensor), there may be too many degrees of freedom to determine if any improvements (or lack thereof) in the RMS are actually a result of modeling physical effects (like correcting for an unmodeled thermal effect) or if it is simply the result of adding more terms.

Model Name	RMS	POP STD
Standard model	4.38	4.54
Standard mod., no aux.	5.63	5.77
Standard mod., no track terms	5.28	5.42
Standard mod., no Constantikes temps.	5.24	5.37
Standard mod. with raw temperature sensors	4.34	4.83
Standard mod. with raw temperature sensors but no Constantikes temps	4.34	4.79
Standard mod. with raw temp sensors and raw incl.'s	4.21	4.77
Standard mod. with raw incl.'s	4.18	4.39
Standard Model minus four aux. terms	4.32	4.46
Standard Model, MVET'ed	4.26	4.38
P1 – no aux, some geom.	4.99	5.13
P2 – no aux, more geom.	4.70	4.86
P3 – some aux, some geom.	3.94	4.08
P4 – more aux., more geom.	4.39	4.59

Table 4. Summary of relative all-sky pointing performance of models on 2017-2018 data sets. Note RMS = root mean square and POP STD = population standard deviation.

4. COMPARISON OF POINTING MODELS' PERFORMANCE ON 2021 DATA

Once we created this set of pointing models by fitting to the 2017-2018 data set, we attempted to determine how well the models would perform on a pointing run which was not included in the set used to create the models. David Frayer conducted a pointing observation on 10 January 2021, TPTCSPNT_211010³, with 58 valid pointings. We selected the night-time pointings from this data set (52 out of the original 58), and after performing the same pre-processing steps on this data set as outlined in section 2, we used TPOINT to apply each model to the 2021 pointing run. Note that we kept all of the coefficients in these models fixed to the values we obtained when fitting them to the 2017-2018 data set with the exception of the terms IE and CAL (or CA, in the case of Patrick Wallace's models); we allowed TPOINT to determine the best values for IE and CAL to simulate local pointing corrections at the beginning of an observing run. Table 5 records the all-sky relative pointing performance of each new model on the 2021 data set.

5. CONCLUSIONS

To compare each of the new models with each other and with the original GBT 5s model, it is necessary to run a series of F-Tests to determine which model(s) achieve the best performance given the number of terms they utilize. The results of these tests suggest that the best model so far of those presented here is the MVET'ed Standard Model. However, it is also apparent that we need to apply the models to more pointing data to compare their performance more rigorously. An area for future work would be to gather more data over a wide range of conditions

³ Commissioning history entry: https://safe.nrao.edu/wiki/bin/view/GB/PTCS/TPTCSPNT_210110

Model Name	RMS	POP STD
Standard model	5.40	5.50
Standard mod., no aux.	6.87	7.01
Standard mod., no track terms	6.35	6.47
Standard mod., no Constantikes temps.	6.01	6.13
Standard mod. with raw temperature sensors	11.58	11.81
Standard mod. with raw temperature sensors but no Constantikes temps	10.63	10.84
Standard mod. with raw temp sensors and raw incl.'s	12.75	13.00
Standard mod. with raw incl.'s	7.38	7.53
Standard mod. minus four aux. terms	5.84	5.95
Standard mod., MVET'ed	5.06	5.16
P1 – no aux, some geom.	7.15	7.29
P2 – no aux, more geom.	6.27	6.39
P3 – some aux, some geom.	6.79	6.93
P4 – more aux., more geom.	5.82	5.94

Table 5. Summary of relative all-sky pointing performance of models on 2021 data set, applied with all coefficients fixed except for IE and CAL. Note, as before, that RMS = root mean square and POP STD = population standard deviation.

and apply each of these new models to this larger data set, and perform a new series of F-tests to assess their performance relative to one another at an improved level of significance.

6. ACKNOWLEDGEMENTS

The authors would like to thank Richard Prestage for his contributions to this project and for his efforts developing, maintaining, and improving the pointing model through the years. We would also like to recognize Kim Constantikes for his substantial role in the creation of the pointing model.

References

- [1] E White et al. “Green Bank Telescope: Overview and analysis of metrology systems and pointing performance”. In: *Astronomy & Astrophysics* (2021).
- [2] Amy Shelton. *GFM Peak and Focus Acceptance Criteria and Heuristics*. URL: <https://safe.nrao.edu/wiki/bin/view/GB/Data/GbtFitsMonitorHeuristics>. (accessed: 08.28.2019).
- [3] Patrick Wallace. *Tpoint: A Telescope Pointing Analysis System, Version 21.8*. 2016.
- [4] Kim Constantikes. “Thermally-neutral traditional pointing models and thermal corrections to pointing and focus”. In: *NRAO Green Bank PTCS Project Note 25* (2007).

TPOINT Coeff. Label	Antenna Manager Coeff. Label	Coordinate	Functional Form	Description
CAL	AZ_D00	$\Delta AZ \cos(EL)$	constant	Cross-elevation offset
HSCE	AZ_D01	$\Delta AZ \cos(EL)$	$\cos(EL)$	Azimuth encoder offset
HSSE	AZ_B01	$\Delta AZ \cos(EL)$	$\sin(EL)$	Azimuth / elevation nonperpendicularity
HSSASE	AZ_A11	$\Delta AZ \cos(EL)$	$\sin(AZ) * \sin(EL)$	North-South tilt of azimuth axis
–HSCASE	AZ_B11	$\Delta AZ \cos(EL)$	$\cos(AZ) * \sin(EL)$	East-West tilt of azimuth axis
–IE	EL_D00	ΔEL	constant	Elevation encoder offset
–HESA	EL_C10	ΔEL	$\sin(AZ)$	East-West tilt of azimuth axis
HECA	EL_D10	ΔEL	$\cos(AZ)$	North-South tilt of azimuth axis
–HESE	EL_B01	ΔEL	$\sin(EL)$	Asymmetric gravity term
–HECE	EL_D01	ΔEL	$\cos(EL)$	Symmetric gravity term
–A12E	The Lambda 1 Track Table values are equivalent to $A12E * \lambda_1$	ΔEL	λ_1	Track term
A13V	The Lambda 2 Track Table values are equivalent to $A13V * \lambda_2 * \sin(EL)$	$\Delta AZ \cos(EL)$	$\lambda_2 * \sin(EL)$	Track term
A14A	The Lambda 3 Track Table values are equivalent to $A14A * \lambda_3 * \cos(EL)$	$\Delta AZ \cos(EL)$	$\lambda_3 * \cos(EL)$	Track term
A2S	az2_2	$\Delta AZ \cos(EL)$	τ_2	Horizontal feedarm and el. bearings (thermal)
A3S	az2_3	$\Delta AZ \cos(EL)$	τ_3	Backup structure and el. bearings (thermal)
A4S	az2_4	$\Delta AZ \cos(EL)$	τ_4	Vertical feedarm (thermal)
–A5E	el_1	ΔEL	τ_5	Backup structure (thermal)
–A6E	el_2	ΔEL	τ_6	Horizontal feedarm and el. bearings (thermal)
–A7E	el_3	ΔEL	τ_7	Vertical feedarm (thermal)
–A8E	el_4	ΔEL	τ_8	Alidade (thermal)
–A9E	el_5	ΔEL	τ_9	Structural temperature average (thermal)
A10V	az2_5	$\Delta AZ \cos(EL)$	$\tau_{10} * \sin(EL)$	Alidade and elevation bearings (thermal)
A11A	az2_6	$\Delta AZ \cos(EL)$	$\tau_{11} * \cos(EL)$	Alidade thermal term

Table 6. This table summarizes the coefficients in the GBT 5s pointing model and their corresponding functional forms [1]. Here, EL stands for mount elevation and AZ for mount azimuth (reckoned north through east), and corrections are encoder minus sky. These are GBT’s conventions, which are different from TPOINT’s, and in order to reproduce this model in a TPOINT session those terms in Column 1 that have a minus must have the GBT coefficient sign reversed. The coefficient labels used in the GBT Antenna Manager that correspond to each TPOINT coefficient are listed in Column 2.

Sensor #	Label	Location of sensor
1	TA1	Alidade: right front
2	TA2	Alidade: left front
3	TA3	Alidade: right rear
4	TA4	Alidade: left rear
5	TE1	Elevation bearing: right
6	TE2	Elevation bearing: left
7	TH2	Horizontal feedarm: right
8	TH1	Horizontal feedarm: left
9	TB1	Backup structure vertex: right
10	TB4	Backup structure: center right
11	TB3	Backup structure: center left
12	TB2	Backup structure vertex: left
13	TB5	Backup structure: center
14	TF2	Vertical feedarm: right front
15	TF3	Vertical feedarm: right rear
16	TF5	Vertical feedarm: left rear
17	TF4	Vertical feedarm: left front
18	TF1	Feedarm tip
19	TSR	Subreflector

Table 7. GBT temperature sensors [4, 1]

Label	Associated TPOINT coefficient	Thermal correction
τ_2	A2S	$(TH2 - TE1)/2.0 - (TH1 - TE2)/2.0$
τ_3	A3S	$(TB1 + TB4 - TB2 - TB3)/2.0 - TE1 + TE2$
τ_4	A4S	$(TF2 + TF3)/2.0 - (TF4 + TF5)/2.0$
τ_5	A5E	$(TB3 + TB4 + TB5)/3.0 - (TB1 + TB2)/2.0$
τ_6	A6E	$(TH2 - TE1)/2.0 + (TH1 - TE2)/2.0$
τ_7	A7E	$(TF2 + TF4)/2.0 - (TF3 + TF5)/2.0$
τ_8	A8E	$(TA1 + TA2)/2.0 - (TA3 + TA4)/2.0$
τ_9	A9E	Average structural temperature
τ_{10}	A10V	$(TA2 + TA3 + TE2 - TA1 - TA4 - TE1)/3.0$
τ_{11}	A11A	$TA4 - TA1 - TA3 + TA2$

Table 8. Temperature correction calculations for each term [4, 1].

Label	Coordinate	Calculation
λ_1	ΔEL	$(X1 + X2)/2$
λ_2	ΔX_EL	$-(Y1 + Y2)/2$
λ_3	ΔX_EL	$(X2 - X1)$

Table 9. Track correction terms. Note that X1 and Y1 are the measurements taken by the inclinometer on the right-hand side of the elevation bearing as you are facing the GBT, whereas X2 and Y2 were taken by the inclinometer on the left. X1, X2, Y1, and Y2 are determined from yearly track measurements in which the inclinometer readings are tabulated as a function of azimuth, therefore the λ values also depend on azimuth [1].

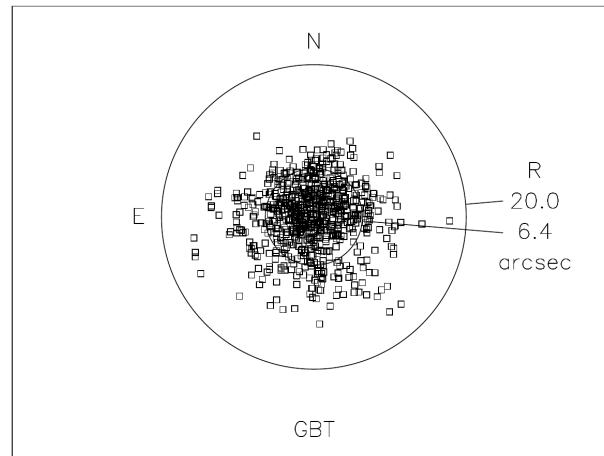


Figure 1. Pointing performance of the GBT's standard (5s) pointing model on the 2017-2018 dataset, given fixed offsets (this simulates blind pointing performance).

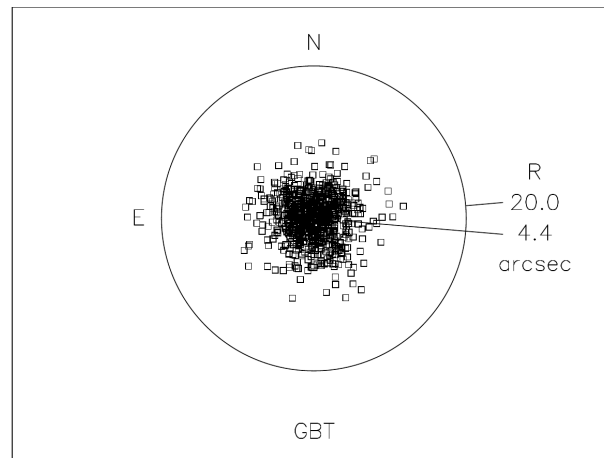


Figure 2. Pointing performance of the GBT's standard (5s) pointing model on the 2017-2018 dataset, with offsets fit to each session (this simulates all-sky relative pointing performance).

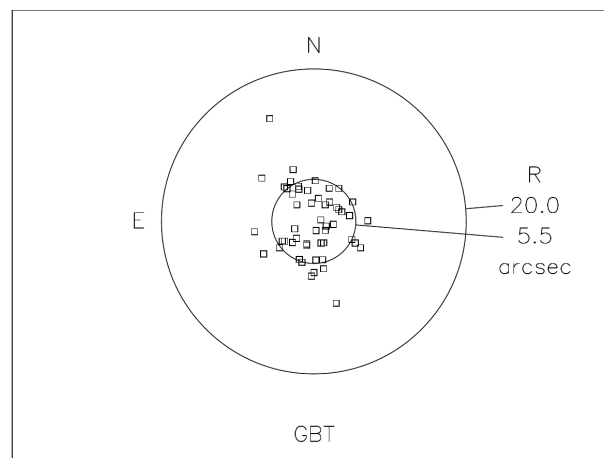


Figure 3. Pointing performance of the GBT's standard (5s) pointing model on the 2021 dataset, with CAL and IE offsets fit to the session (this simulates all-sky relative pointing performance).

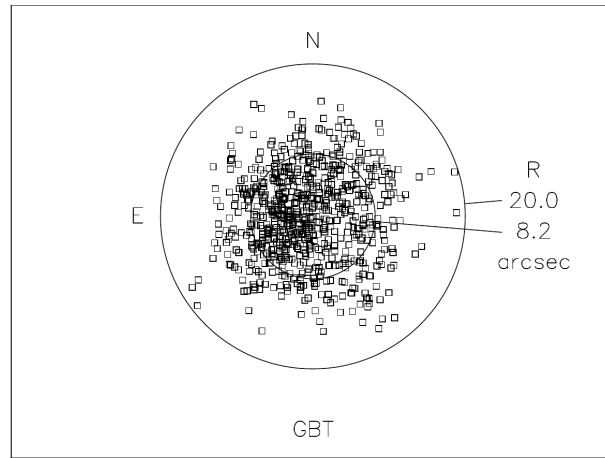


Figure 4. Pointing performance of the MVET'ed pointing model on the 2017-2018 dataset, given fixed offsets (this simulates blind pointing performance).

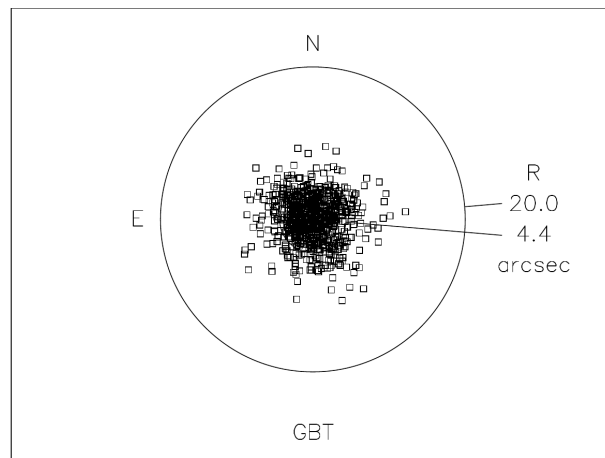


Figure 5. Pointing performance of the MVET'ed pointing model on the 2017-2018 dataset, with offsets fit to each session (this simulates all-sky relative pointing performance).

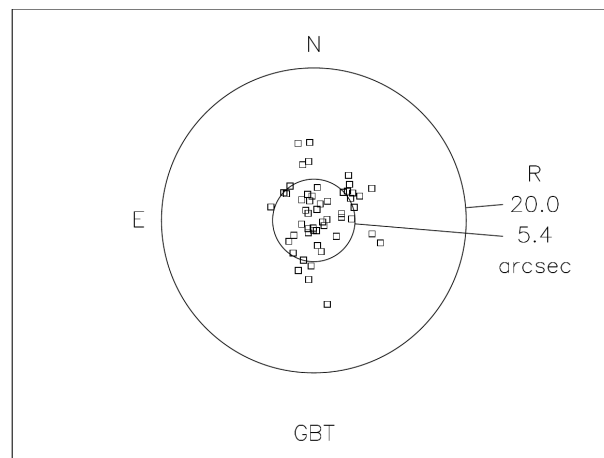


Figure 6. Pointing performance of the MVET'ed pointing model on the 2021 dataset, with CAL and IE offsets fit to the session (this simulates all-sky relative pointing performance).